# Propiedades ópticas y químicas de las fracciones de material particulado atmosférico relacionadas con las masas de aire en el centro de la Península Ibérica

## Optical and chemical properties of atmospheric PM fractions related with air masses in the central Iberian Peninsula

S. Mogo [1,2], V. E. Cachorro [1], M. Sorribas[1], A. M. de Frutos [1]

1. Departamento de Física Teórica, Atómica y Óptica, Grupo de Óptica Atmosférica, Facultad de Ciencias, Universidad de Valladolid, Valladolid, España.
2. Departamento de Física, Universidade da Beira Interior, Covilhã, Portugal. Email: smogo@ubi.pt

## RESUMEN

Entre diciembre de 2003 y junio de 2004 se han tomado muestras aproximadamente semanales en Valladolid, España. Se han realizado medidas gravimétricas de las 4 fracciones de material particulado: PST, PM10, PM2.5 y PM1. Las muestras se han analizado por cromatografía iónica. Las propiedades ópticas de la fracción fina se estudian por medio de los coeficientes de absorción, $\sigma_a$, en el rango visible y la forma espectral de $\sigma_a$ se analiza derivando un parámetro $\alpha_a$ análogo al exponente de Ångström utilizado para la extinción. Las propiedades de los aerosoles se clasifican de acuerdo con la dependencia del origen de las masas de aire.

**Palabras clave:** Partículas y aerosoles, Absorción de la radiación, Atmósfera.

## ABSTRACT

From December 2003 to June 2004 approximately weekly aerosol samples were collected in Valladolid, Spain. Gravimetric measurements were performed on the four particulate matter fractions: TSP, PM10, PM2.5 and PM1. The samples were analyzed for major ions by ion-chromatography. The optical properties of the fine particles are studied through the absorption coefficients, $\sigma_a$, in the visible range and the spectral shape of $\sigma_a$ was analyzed by deriving a parameter, $\alpha_a$, similar to the Ångström exponent used for the extinction. Aerosol properties are classified according to their dependence on air mass origin.

**Key words:** Particles and aerosols, Absorption of radiation, Atmosphere.

## REFERENCIAS Y ENLACES

[1] J. Haywood, O. Boucher, "Estimates of direct and indirect radiative forcing due to tropospheric aerosols: a review", *Rev. Geophys.* **38**, 513-543 (2000).

[2] R. Van Dingenen, F. Raes, J.-P. Putaud, U. Baltensperger, A. Charron, M.-C. Facchini, S. Decesari, S. Fuzzi, R. Gehrig, H.-C. Hansson, R. M. Harrison, C. Hüglin, A. M. Jones, P. Laj, G. Lorbeer, W. Maenhaut, F. Palmgren, X. Querol, S. Rodriguez, J. Schneider, H. ten Brink, P. Tunved, K. Tørseth, B. Wehner, E. Weingartner, A. Wiedensohler, P. Wåhlin, "A European aerosol phenomenology 1: physical characteristics of particulate matter at kerbside, urban, rural and background sites in Europe", *Atmos. Environ.* **38**, 2561-2577 (2004).

[3] J.-P. Putaud, F. Raes, R. Van Dingenen, E. Büggemann, M.-C. Facchini, S. Decesari, S. Fuzzi, R. Gehrig, C. Hüglin, P. Laj, G. Lorbeer, W. Maenhaut, N. Mihalopoulos, K. M¨ller, X. Querol, S. Rodriguez, J. Schneider, G. Spindler, H. Brink, K. Tørseth, A. Wiedensohler, "A European aerosol phenomenology 2:

 © Sociedad Española de Óptica

chemical characteristics of particulate matter at kerbside, urban, rural and background sites in Europe", *Atmos. Environ.* **38**, 2579-2595 (2004).

[4] K. Willeke , P. Baron, Editors, *Aerosol Measurement. Principles, Techniques, and Applications*. John Wiley & Sons Inc. (1993).

[5] R. Cuddihy, W. Griffth, O. McClellan, "Health risks for light duty diesel vehicles", *Environ. Sci. Technol.* **18**, 14A-21A (1984).

[6] D. Encinas, H. Casado, J. Lacaux, P. van Dinh, "Concentration and size distribution of atmospheric particulate matter on a forested area in the Basque Country (SPAIN)", *J. Environ. Sci. Heal. A* **29**, 99-114 (1994).

[7] C. Pope, R. Burnett, M. Thun, E. Calle, D. Krewski, K. Ito, G. Thurston, "Lung cancer, cardiopulmonary mortality, and long-term exposure to fine particulate air pollution", *J. Am. Med. Assn* **287**, 1132-1141 (2002).

[8] H. Horvath, "Atmospheric light absorption - a review", *Atmos. Environ.* **27A**, 293-317 (1993).

[9] O. Dubovik, B. Holben, T. Eck, A. Smirnov, Y. Kaufman, M. King, D. Tanré, I. Slutsker, "Variability of absorption and optical properties of key aerosol types observed in worldwide locations", *J. Atmos. Sci.* **59**, 590-608 (2002).

[10] C. Wang, "A modeling study on the climate impacts of black carbon aerosols", *J. Geophys. Res. D* **109**, D03106 1-28 (2004).

[11] S. Chandra, S. Satheest, J. Srinivasan, "Can the state of mixing of black carbon aerosols explain the mistery of 'excess' atmospheric absorption?", *Geophys. Res. Lett.* **31,** L19109 (2004).

[12] G. Schuster, O. Dubovik, B. Holben, E. Clothiaux, "Inferring black carbon content and specific absorption from Aerosol Robotic Network (AERONET) aerosol retrievals", *J. Geophys. Res.* **110,** D10S17 (2005).

[13] P. Buseck, M. Pósfai, "Airbone minerals and related aerosol particles: Effects on climate and environment", *P. Natl. Acad. Sci. USA* **96**, 3372-2279 (1999).

[14] INM. *Guía resumida del clima en España 1971-2000*, http://www.inm.es (2000).

[15] M. Sánchez, D. Pascual, C. Ramos, and I. Pérez, "Forecasting particulate pollutant concentrations in a city from meteorological variables and regional weather patterns", *Atmos. Environ.*, **24A**(6), 1509-1519 (1990).

[16] C. Toledano. *Climatología de los aerosoles mediante la caracterización de propiedades ópticas y masas de aire en la estación 'El Arenosillo' de la red AERONET*, PhD Thesis, Universidad de Valladolid (2005).

[17] S. Mogo, V. Cachorro, A. de Frutos, "Morphological, chemical and optical absorbing characterization of aerosols in the urban atmosphere of Valladolid", *Atmos. Chem. Phys.* **5**, 2739-2748 (2005).

[18] C. Lin, M. Baker, R. Charlson, "Absorption coefficient of atmospheric aerosol: a method of measurement", *Appl. Opt.* **12**, 1356-1363 (1973).

[19] H. Horvath, "Experimental calibration for aerosol light absorption measurements using the integrating plate method - summary of the data", *J. Aerosol Sci.* **28**, 1149-1161 (1997).

[20] T. Bond, T. Anderson, D. Campbell, "Calibration and intercomparison of filter-based measurements of visible light absorption by aerosols", *Aerosol Sci. Tech.* **30**, 582-600 (1999).

[21] B. Bodhaine, "Aerosol absorption measurements at Barrow, Mauna Loa and the South Pole", *J. Geophys. Res.* **100**, 8967-8975 (1995).

[22] P. Fialho, A. Hansen, R. Honrath, "Absorption coefficients by aerosols in remote areas: a new approach to decouple dust and black carbon absorption coefficients using seven-wavelength aethalometer data", *J. Aerosol Sci.*, **36**, 267-282 (2005).

[23] EMEP. EMEP/CCC-Report 4/2002: Measurements of Particulate Matter: Status Report 2002. Technical report, M. Kahnert, Norwegian Institute for Air Research (2002).

[24] X. Querol, A. Alastuey, M. Viana, S. Rodriguez, B. Artiñano, P. Salvador, S. Santos, R. Patier, C. Ruiz, J. de la Rosa, A. de la Campa, M. Menendez, J. Gil, "Speciation and origin of PM10 and PM2.5 in Spain", *J. Aerosol Sci.* **35**, 1151-1172 (2004).

[25] A. Sánchez de la Campa. *Geoquímica del material particulado atmosférico en Huelva, Suroeste de España*. PhD Thesis, Universidad de Huelva (2004).

[26] A. Vázquez, M. Costoya, R. Peña, S. García, C. Herrero, "A rainwater quality monitoring network: a preliminary study of the composition of rainwater in Galicia (NW Spain)", *Chemosphere*, **51**, 375-386 (2003).

 © Sociedad Española de Óptica

[27] H. Casado, D. Encinas, J. Lacaux, "Relationship between the atmospheric particulate fraction and the ionic content of precipitation in an area under influence of a waste incinerator located in the Basque Country (Spain)", *Atmos. Environ.* **30**, 1537-1542 (1996).

[28] C. Chou, T.-K. Chen, S.-H. Huang, S. Liu, "Radiative absorption capability of Asian dust with black carbon contamination", *Geophys. Res. Lett.*, **30**, 18-1 (2003).

[29] J. Heintzenberg, M. Bussemer, "Development and application of a spectral light absorption photometer for aerosol and hydrosol samples", *J. Aerosol Sci.* **31**, 801-812 (2000).

[30] W. Arnott, H. Moosmüller, P. Sheridan, J. Ogren, R. Raspet, W. Slaton, J. Hand, S. Kreidenweis, J. Collett Jr, "Photoacoustic and filter-based ambient aerosol light absorption measurements: Instrument comparisons and the role of relative humidity", *J. Geophys. Res. D* **108**, AAC15 1-11 (2003).

[31] S. Mogo, V. Cachorro, M. Sorribas, A. de Frutos, R. Fernández, "Measurements of continuous spectra of atmospheric absorption coefficients from UV to NIR via optical method", *Geophys. Res. Lett.* **2**, L13811 (2005).

[32] T. Kirchstetter, T. Novakov, P. Hobbs, "Evidence that the spectral dependence of light absorption by aerosols is affected by organic carbon", *J. Geophys. Res.* **109**, D21208 (2004).

[33] B. Bodhaine, J. Harris, J. Ogren, and D. Hofmann, "Aerosol optical properties at Mauna Loa Observatory: Long-range transport from Kuwait?", *Geophys. Res. Lett.*, **19**, 581-584 (1992).

[34] C. Liousse, H. Cachier, S. Jennings, "Optical and thermal measurements of black carbon content in different environments: variation of specific attenuation cross-section", *Atmos. Environ.* **A27**, 1203-1211 (1993).

[35] J. Martins, P. Hobbs, R. Weiss, P. Artaxo, "Sphericity and morphology of smoke particles from biomass burning in Brazil", *J. Geophys. Res.* **103**, 32,051-32,067 (1998).

[36] R. Draxler, G. Rolph, (HYbrid Single-Particle Lagrangian Integrated Trajectory) Model access via NOAA ARL READY Website (http://www.arl.noaa.gov/ready/hysplit4.html). NOAA Air Resources Laboratory, Silver Spring, MD (2003).

[37] G. Rolph, Real-time environmental applications and display system (ready) website (http://www.arl.noaa.gov/ready/hysplit4.html). NOAA Air Resources Laboratory, Silver Spring, MD, (2003).

## 1. Introduction

Studies of atmospheric aerosols have increased in the last decades not only due to their influence on climate by "radiative forcing" [1-3] but also due to air quality control [4]. In either case, the studies are not only focused in aerosols of anthropogenic origin but also in those of natural origin as desertic or maritime. The atmospheric amount of particulate matter (PM) has become a key factor, in part due to the harmful effects of some aerosols on human health [5-7] and the close relationship between aerosols and air pollution.

It is convenient to split the properties of aerosols into two main classes, physico-chemical properties and optical or radiative properties. The first class is associated to the aerosol size, morphology, structure and composition. This class is the main focus of atmospheric pollution and air quality studies. The second class is relevant for the interaction effects of aerosols with solar and terrestrial radiation, through the processes of absorption and scattering, leading to a radiation extinction coefficient and to the aerosols optical depth after vertical integration. Other relevant parameters are the single scattering albedo and the asymmetry parameter [8,9].

The net effect of aerosols on the climate is still not completely clear, despite the huge number of studies about their radiative properties. Atmospheric aerosols can behave as a factor of cooling or warming, depending in what prevails [10]: the light absorption or the scattering (that is to say the single scattering albedo). The elemental composition is one of the factors that, among others, influence the scattering and absorption of light by particles. Sulphates are the main type of aerosols leading to a net cooling by scattering solar radiation and are very effective as cloud condensation nuclei. This results in a negative radiative forcing that leads to a cooling effect on the Earth surface. On the contrary, soot, mainly composed of carbon particles is considered the greater absorber of solar radiation and has, therefore, a warming effect.

Particle scattering and absorption properties depend not only on the individual radiative properties of the particles (such as shape, complex refractive index, size parameter, size distribution, wavelength of the incident light) but also on how the

 © Sociedad Española de Óptica

various aerosol species are mixed. The particles state of aggregation, that is, if they form an internal mixture, an external mixture or a core-shell structure, is also an important factor. If a particle is mixed internally with other particles, their optical properties can vary [11,12]. For example, a soot inclusion in a sulphate particle changes the optical properties of the sulphate. If the sulphate particle is alone its effect is a net cooling of the atmosphere; but, if contains sufficient soot it can emit infrared radiation and hence warm the surrounding atmosphere. Usually, the absorption coefficient of a mixture of elemental carbon with non-absorbent particles, is higher for an internal mixture than for an external one [8]. Hence, knowledge of the radiation scattering and absorption properties of the atmospheric aerosol is of utmost importance but, studies of the aerosols optical and radiative characteristics should not be carried out without also considering its chemical composition.

Bearing in mind that anthropogenic aerosols have, in general, the greatest impact on the climate near their sources [10,13], this work is focused on the analysis of particles found in the atmosphere of the city of Valladolid (Spain) in order to categorize the chemical constitution of its components, and also its absorbent characteristics, which are directly related to its range of sizes. It does not intend to be a monitoring study for Valladolid but only identify the main components of the local PM and relate it with the optical parameters measured.

## 2. Experimental

### 2.a. Sampling location

The particles sampled in this study were collected within the urban environment of Valladolid, Spain (41.67N, 4.74E), during 2004 winter and spring. Valladolid is a medium size town with ≈ 500.000 inhabitants located in the north-center of the Iberian Peninsula (continental climate), Fig. 1. The urban aerosol corresponds to a not very industrialized city, whose pollution basically arises from road traffic and domestic heating, and is strongly dependent of the weather and atmospheric conditions. The continental climate of the region is characterized by short and very hot summers and long and cold winters with very frequent fog, due to the Pisuerga River Valley that crosses the city. The relative humidity goes from 83% in January to 54% in June, the annual mean being ca. 65%. Precipitation varies from 40 mm in January to 33 mm in June, the annual mean is 435 mm (data from the INM (2000) [14]). The predominant wind direction follows the river valley, NE-SW, however approximately 25% of the days have calm wind. Synoptic meteorological classification and its relationship with particulate matter concentration had been established before [15] and identified two characteristic situations: high pollution events corresponding with anticyclonic weather and very low pollution levels corresponding to air masses coming from the Arctic. Extremely high episodes of particle concentration occur during Saharan desert dust intrusions which are very frequent. Although there is no specific inventory about Valladolid, there is an incidence of 14%-21% of the days per year with desertic dust intrusions in south Spain [16] and most of them should reach Valladolid.

The sampling site was in the campus of Valladolid University and the impactor was located on a balcony on the second floor of the building of Sciences Faculty, ≈ 150 m from the nearest street.

In the bibliography, only optical data can be found about this town [17] or others in this part of the Iberian Peninsula which is a mostly uncharacterized region.


Fig. 1. Map of the area. The arrows indicate the main origins of air masses that usually arrive at the Iberian Peninsula. Air masses passing over the Mediterranean sector have a very low incidence and are included together with the continental ones coming from Europe.

### 2.b. Aerosol collection

A Dekati PM10 impactor collecting over polycarbonate membrane filters with 0.2 μm pores was used, working with a constant flow rate of 16.5 l/min. The impactor is composed of four stages and the aerodynamic cut-off diameters are 1 μm, 2.5 μm and 10 μm, allowing the description of four fractions of particulate matter in the ranges < 1 μm, 1-2.5 μm, 2.5-10 μm and > 10 μm.

A total of 16 days and 64 filters were analyzed from Dec 2003 to Jun 2004 on a weekly basis. The sampling took place during the night, starting at local 08:00 pm and the sampling times varied from 8

 © Sociedad Española de Óptica

to 15 h. Sampling interval times were limited by the amount of aerosol needed by the integrating plate technique for the evaluation of the absorption coefficient of particles smaller than 1 μm.

The filters were weighed before and after collection, and care was taken to eliminate electrostatic charges from them before weighing.

### 2.c. Optical analysis: absorption coefficients determination

The absorption coefficients were evaluated by performing measurements on every filter before and after the aerosol collection. The method used is an adaptation of the integrating plate method [18-20] and is fully described in Mogo *et al* [17].

The aerosol absorption coefficients ($\sigma_a$) of particle samples with aerodynamic size below 1 μm were determined by:

$$\sigma_a(\lambda) = -\frac{A}{V}\ln\left(\frac{I_f(\lambda)}{I_0(\lambda)}\right), \qquad (1)$$

where $I_f(\lambda)$ and $I_0(\lambda)$ are the intensities of light passing through the sampling filter and a blank filter, respectively, for each wavelength, $V$ is the volume of sampled air and $A$ is the effective cross-section area of the filter.

Since we have detailed spectral information, a reliable analysis of the spectral shape of the absorption coefficient can be carried out. In order to evaluate the slope of the absorption spectra we use an equivalent coefficient commonly used in aerosol extinction studies, the Ångström exponent. As already proposed by other authors [21,22], we use the empirical expression:

$$\sigma_a(\lambda) = K\left(\frac{\lambda}{\lambda_0}\right)^{-\alpha_a}, \qquad (2)$$

where $K$ is a constant (with the same units as $\sigma_a$), $\lambda$ is the wavelength, $\lambda_0$ is an arbitrary reference wavelength usually taken as 1 μm and $\alpha_a$ is the absorption alpha exponent which represents the aerosol size and refractive index influence on the wavelength. This power law expression characterizes the steepness of the slope of the curve $\sigma_a$ *versus* $\lambda$.

The mass absorption specific coefficient of fine particles, $B_a(\lambda)$ can be obtained from:

$$B_a(\lambda) = \sigma_a(\lambda)\cdot\left[M\phi < 1\,\mu\mathrm{m}\right]^{-1}, \qquad (3)$$

where $M\phi < 1$ μm is the mass concentration of submicrometric particles.

Using this method we assume that the optical properties of the particles are not altered by the collection method and that their behavior remains the same after being collected in the filter as it would be in an atmosphere cylinder of thickness $x$ and section equal to the filter's effective cross-section, $A$.

### 2.d. Chemical analysis and microanalysis of samples

After the determination of absorption coefficients, as the technique used is non-destructive, the samples were analyzed for major ions using ion chromatography. The filters were treated with deionised water and the soluble matter ultrasonically extracted. Samples were placed in the ultrasound bath for half an hour. Then, levels of $Cl^-$, $NO_3^-$, $SO_4^{2-}$, $Mg^{2+}$, $Ca^{2+}$, $K^+$, $Na^+$ and $NH_4^+$ were assayed by means of ionic chromatography with conductometric detection [6]. This procedure allowed the mass ions of the four well established sizes to be obtained. The average error in the measurements does not exceed 5%.

As a complementary analysis, some representative samples were selected for morphologic and elemental analysis of single particles by scanning electron microscopy (SEM) and energy dispersive X-ray (EDX). The results have already been presented elsewhere [17] and will not be discussed here except to confirm some results about particle chemical composition.

## 3. Results and discussion

### 3.a. PM levels and components

The PM10 values registered range from 25.06 μg/m$^3$ to 138.93 μg/m$^3$ and the average for all measured days is 75.26 μg/m$^3$. Figure 2 shows time series of the mass concentrations of TSP, PM10, PM2.5 and PM1, the mean values are summarized in Table I. Although these values were obtained during only a short campaign, Table I clearly reflects that they are very high, but high values had already been reported in Spanish stations [23]. According to Querol *et al* [24], 60% of the PM10 mass and 60-70% of the PM2.5 mass is attributed to regional background in which soils have considerable contribution.

The contribution of PM1, PM1-2.5 and PM2.5-10 in PM10 is presented in Fig. 2(a). The PM2.5-10 contribution in the PM10 mass is ≈ 35%, which is within the range presented by Querol *et al* [24] for central and north Spain but the load of PM1 in PM10 (≈36%) is below their values. Nevertheless, the values presented by Querol *et al* [24] for central and north Spain are representative of rural (Bemantes) and/or urban background (Llodio) and they are not comparable with the urban atmosphere

 © Sociedad Española de Óptica

of Valladolid. Our values are representative of a urban medium-sized town in Spain, a continental central site in the Iberian Peninsula, where the PM levels are, as yet, not well established, The high correlation of PM2.5 to PM10 with a slope of 0.65 (R=0.98) is indicative of the dominance of coarse particles to fine particles [2,25], as confirmed by the C/F ratio, between particles with diameter 1-10 μm and submicrometric particles. This ratio is presented in Fig. 3 together with the time series of PM1 and PM1-10 (see also Table I) showing the bimodal feature which generally characterizes size distribution of ambient aerosol. The submicrometric mode is usually associated with air pollution whereas the larger mode mostly consists of dust and mineral soil particles. The submicrometric particles concentration ranged between 10.23 μg/m$^3$ and 53.60 μg/m$^3$, the average value was 28.22 μg/m$^3$. The concentration of particles 1-10 μm ranged between 7.66 μg/m$^3$ and 85.77 μg/m$^3$, its average value was 47.04 μg/m$^3$. The ratio C/F was generally larger than 1.0 during the period of measurement, thus the presence of larger particles seems to be a characteristic of the Valladolid atmosphere.

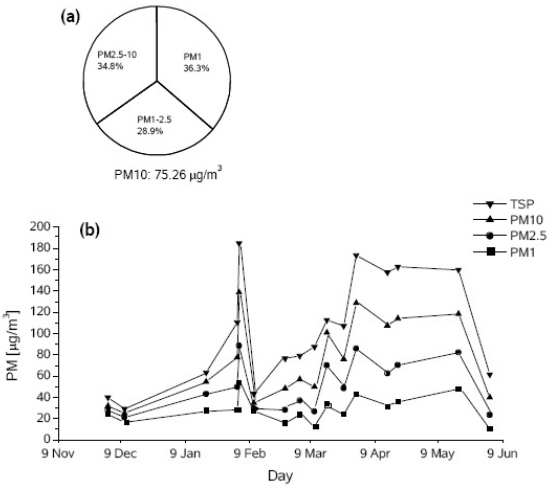


Fig. 2. (a) Mean mass contributions of PM1, PM1-2.5 and PM2.5-10 in PM10. (b) Concentrations of aerosols observed during the measurement period.

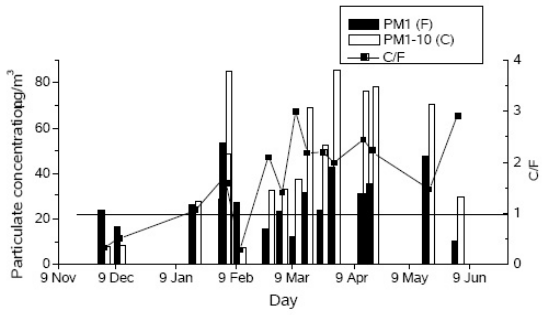


Fig. 3. Concentrations of the observed aerosols and ratio C/F.

In Fig. 4 the average concentration of anions and cations in each impactor stage is shown. Sulphate and nitrate are important contributors to the PM mass concentration and the aerosol found in Valladolid has significant levels of $Na^+$. The $Mg^{2+}$ and $NH_4^+$ ions come next in the scale. The average concentration for the remaining ions is less relevant. These results are comparable with those described for the city centre of other towns [3]. Table I summarizes the mean daily levels of TSP, PM10, PM2.5, PM1, BC and major ionic components during the measurement period. Figure 5 shows the averaged relative contributions of various species to each PM fraction. All components are present in both the fine and the coarse fractions, but their contributions in each fraction are different.

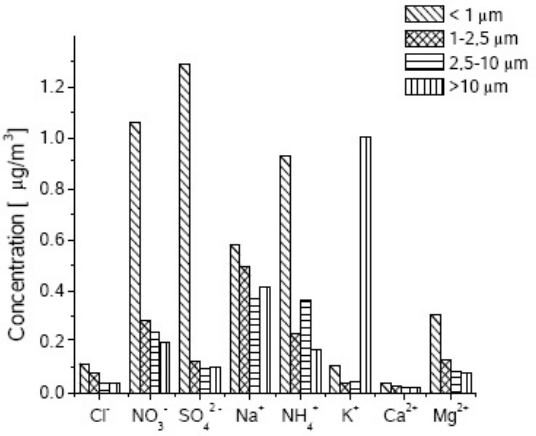


Fig. 4. The average concentration of anions and cations of aerosol particles for each impactor stage.

Table I. Mean levels of TSP, PM10, PM2.5, PM1, BC and major ionic components measured at Valladolid.

| | PM1 | PM2.5 | PM10 | TSP |
|---|---|---|---|---|
| | | μg/m$^3$ | | |
| PM | 28.22 | 49.64 | 75.26 | 108.03 |
| BC | 3.77 | - | - | - |
| $SO_4^{2-}$ | 1.29 | 1.41 | 1.51 | 1.61 |
| $NO_3^-$ | 1.06 | 1.34 | 1.58 | 1.77 |
| $Cl^-$ | 0.11 | 0.19 | 0.23 | 0.27 |
| $Na^+$ | 0.58 | 1.08 | 1.45 | 1.87 |
| $NH_4^+$ | 0.93 | 1.16 | 1.52 | 1.69 |
| $K^+$ | 0.10 | 0.14 | 0.19 | 1.19 |
| $Ca^{2+}$ | 0.04 | 0.07 | 0.08 | 0.10 |
| $Mg^{2+}$ | 0.31 | 0.43 | 0.52 | 0.59 |

 © Sociedad Española de Óptica

As a typical urban atmosphere, the fine mode is basically composed of $SO_4^{2-}$, $NO_3^-$ and $NH_4^+$ ions which display clearly maximum concentration in stage 0 of the impactor, submicrometric particles. The $Na^+$ ion can be found in approximately the same proportion in the four size levels. Regarding the $K^+$ ion, it is predominantly found in coarse particles. The high concentration of $Na^+$ was confirmed by semiquantitative analysis of samples using a SEM/EDX combined technique [17]. This high concentration of salt has already been reported by other authors [26,27] in reports on rainwater monitoring in other northern Spanish Towns. This may be related the "thaw-salt" used in the streets on winter days to help clear ice and snow.

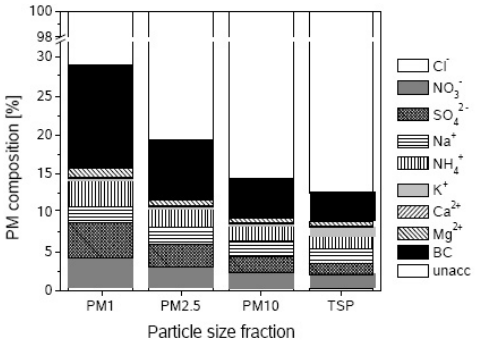


Fig. 5. Averaged chemical composition of the identified portions of PM1, PM2.5, PM10 and TSP. Note that the volatile components are missed with these techniques.

### 3.b. Determination of the absorption coefficient and black carbon content

An important characteristic of the urban atmosphere is its optical absorption properties which are represented by the absorption coefficient. In Fig. 6 the time series of the absorption coefficient for submicrometric particles in visible wavelengths are presented. For 550 nm the minimum and maximum absorption coefficients were 7.3 $Mm^{-1}$ and 101.4 $Mm^{-1}$ respectively. The average value for all the measurement periods was 44.7 $Mm^{-1}$. Our daily detection limit for the absorption coefficient is 0.01 $Mm^{-1}$. The average absorption coefficient measured had a minimum value of 4.6 $Mm^{-1}$ for 650 nm and a maximum of 120.3 $Mm^{-1}$ for 450 nm.

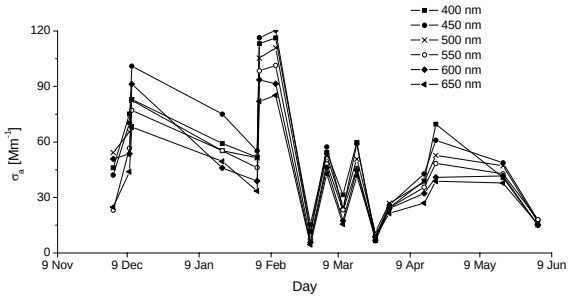


Fig. 6. Time series of the absorption coefficients observed during the measurement period.

The values of the absorption coefficient reported are within the expected range for this urban atmosphere. However, we must emphasize the strong variations observed during the whole experimental period (see February as the period with maximum variations). Values reported by other authors are: 50-250 $Mm^{-1}$ for dust with black carbon contamination in Asia [28], between 5-80 $Mm^{-1}$ for aerosols in Melpitz, Germany [29], a maximum value of 2.1 $Mm^{-1}$ for Big Bend National Park in South Texas, USA [30]. At a rural site in southern Spain ("El Arenosillo" Atmospheric Sounding Station) we measured values between 0.09 $Mm^{-1}$ and 2.31 $Mm^{-1}$ for 550 nm [31].

The variation of the absorption coefficient for 550 nm and the ratio C/F, are shown in Fig. 7. By looking at the shape of the curves it can be observed, a clear anticorrelation between $\sigma_a$ and C/F as, each increase of the absorption coefficient coincides with a decrease of the ratio C/F. The situations of C/F<1.0 coincides with the highest absorption coefficients measured. The increase of the C/F ratio is usually associated with an increase in the levels of the large non-absorbent particles. In this situation, a decrease is registered in the value of the absorption coefficients. On the contrary, when the levels of fine particles increase, the ratio C/F decreases and higher values of $\sigma_a$ are registered. Exceptions to this situation occur in the presence of desert dust intrusions in which the ratio C/F increases but $\sigma_a$ may remain constant or not depending on the level of small absorbent particles not associated with the dust event.

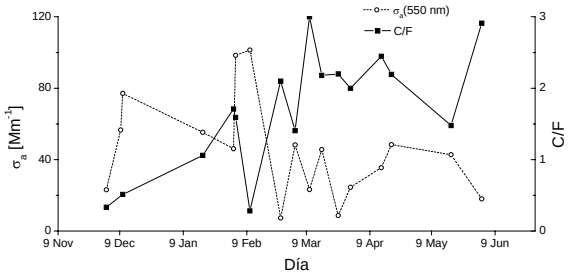


Fig. 7. Variation of absorption coefficient for 550 nm and of the ratio C/F during the period of sampling.

The shape or variation of the $\sigma_a$ through the visible spectrum is carried out by a detailed evaluation of the absorption alpha exponent, $\alpha_a$, which is obtained by linear fitting in the log-log plot of $\sigma_a$ *versus* $\lambda$. The calculated alpha absorption exponents are plotted in Fig. 8. The results are in the range 0.1-1.3 and the average alpha value is 0.7 (standard deviation 0.4). Then the absorption coefficient varies in average with the wavelength according to the law $\lambda^{-0.7}$. When the absorption coefficient does not present any wavelength dependence, the alpha parameter of absorption is

$\alpha_a$=0. The wide range reported is due to the long period of the measurements, where different types of aerosols were collected. The weight fit error associated with the determination of the absorption alpha parameter was determined and reaches, in the worst case, as much as ±30%. The alpha parameter is highly sensitive to the absorption spectral variation and one must be aware of the high uncertainty in the determination of this parameter, and use it with extreme care. The extreme value obtained for 26 Feb, $\alpha_a$=2.5, is considered as not reliable because it refers to very small values of the absorption coefficients. This increases the uncertainty in the determination of the absorption alpha parameter because we approach the limit of detection in the integrating plate system. This value was not considered for the determination of the average $\alpha_a$. In a paper on the influence of organic carbon in the light absorption spectral dependence, Kirchstetter *et al.* [32] used a similar empirical approach and obtained absorption exponents for various fine mode aerosol samples, between 0.6 and 2.9. Bond *et al.* [20] also assumes a similar relation and reported α values in the range 1.7-2.5 for the industrial combustion of lignite. Mogo *et al.* [31] obtained values in the range 0.2-2.0, for the 400-800 nm region at the El Arenosillo site.

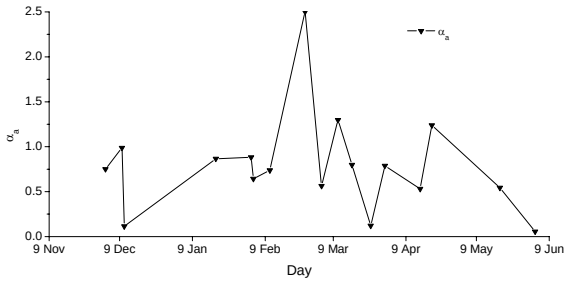


Fig. 8. Evolution of the absorption alpha parameter during the period of measurements. The extreme value of 26 Feb ($\alpha_a$=2.5) is considered as not reliable (see text for explanation).

The time series of the mass specific absorption coefficient of PM1 and PM10 are presented in Fig. 9. For $B_{a(PM1)}$ (550 nm) the values vary between 0.4 $m^2/g$ and 4.7 $m^2/g$, the average value was 1.8 $m^2/g$. For $B_{a(PM10)}$ (550 nm) the values vary between 0.1 $m^2/g$ and 2.8 $m^2/g$, the average value was 0.9 $m^2/g$. The variability of $\sigma_a$ and PM values is reflected in the large range of values obtained for $B_a$, nevertheless, in Fig. 9 it is possible to see winter values are predominantly higher than spring values. We observe that the higher $B_a$ values registered correspond to situations when the concentration of the PM fine fraction was higher than the concentration of the coarse fraction.

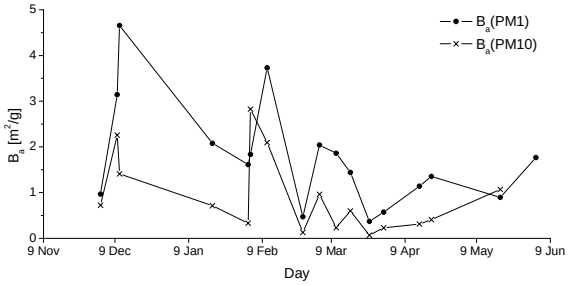


Fig. 9. Evolution of the mass specific absorption coefficient of aerosols for the wavelength of 550 nm during the period of measurements.

If we assume the commonly accepted value of 10 $m^2/g$ for the mass specific absorption coefficient of black carbon [33-35], we can make a rough estimation of the concentration of black carbon, just by putting $B_{a(BC)}$=10 $m^2/g$ in $M_{BC}=\sigma_a(B_{a(BC)})^{-1}$. We used the $\sigma_a$ determined for 650 nm because we have smaller errors for this wavelength. With this approach, the minimum, maximum and average concentration of black carbon observed were, respectively, 0.46 $\mu g/m^3$, 8.52 $\mu g/m^3$, and 3.77 $\mu g/m^3$, see Table I. With this approach we assume that black carbon is the only absorber of light at the wavelengths in which we are working.

### 3.c. Analysis of backward trajectories

Pure aerosol types, marine, continental, desert, etc., are associated with well defined air masses. However different air masses can arrive at a given place giving rise to mixed aerosols and properties variability, thus defining the local aerosol climatology. Therefore the origin of air masses must be analyzed together with its aerosol properties. To achieve this objective we have carried out a backtrajectory analysis using NOAA's HYSPLIT model [36,37]. The backtrajectories were calculated for 5 days at three different altitudes, 500, 1500 and 3000 m above ground level, over Valladolid.

These trajectories for the days of the measuring period were analyzed and classified in order to identify the most common and characteristic local situations. The Atlantic origin includes three different situations: air masses from the Arctic - maritime arctic air mass; air masses from the Atlantic north but not from the Arctic - maritime polar air masses; air masses from lower latitudes that reach the Iberian Peninsula from the west or southwest - maritime tropical air masses. The air masses with European origin usually originated in Siberia or north Europe and are classified as continental because they reach Spain after crossing the European continent or remain in it for enough time in order to allow mixing with local aerosol components. Due to the proximity of the African continent, the Iberian Peninsula is strongly affected

 © Sociedad Española de Óptica

by desert outbreaks. The air masses classified as originating from south Spain and Africa come from the north of the African continent, the Sahara Desert or Sahel Desert.

The air masses were assigned Atlantic origin in ≈47% of the days, central Europe origin in ≈ 29% of the days, southern (south Spain and Africa) in ≈12% of the cases and they arrived from other directions in ≈12% of the days.

Figure 10 summarizes the main characteristics of aerosol optical properties and concentration levels for the four air mass types. The mean values of $\sigma_a$, $B_a$, $\alpha_a$ and PM fraction concentrations, are shown in each of the situations. The most clear situation corresponds to air masses coming from south Spain and Africa. The entry of Saharan dust events is commonly observed in the Iberian Peninsula and is characterized by higher values of the PM and absorption coefficients. The $\alpha_a$ parameter ranges from an average of 0.4 when air masses came from central Europe to 0.84 when they came from the Atlantic. During Saharan dust events, the average $\alpha_a$ was 0.8.

The highest absorption event of the campaign was observed on 12 Feb. The PM levels remain at low values but the C/F ratio is the lower registered, C/F = 0.28, indicating the predominance of fine particles. For this day it was observed that air masses, although of atlantic origin, crossed through heavy industrialized areas of south England and northwest France, entering Spain via the Basque Country. Transport from central Europe is supported by backward trajectory modeling for air parcels arriving at the site, as shown in (a). Air masses originated in central Europe, indicating the advection of the likely anthropogenic pollutants. On the other hand, in (b) the trajectories of air masses on 27 Feb are shown, coinciding with the lower measured absorption coefficient and low PM concentration. Backward trajectories indicate air masses stemming from the Arctic (east from Greenland) and reaching Spain via the north of the country. In (c) another common situation which occurred on 17 Mar is shown, the entry of a Saharan dust event: the air masses arrived from North Africa, the Sahara Desert. The absorption coefficients remain within average values ($\sigma_a$=45.7 $Mm^{-1}$ at

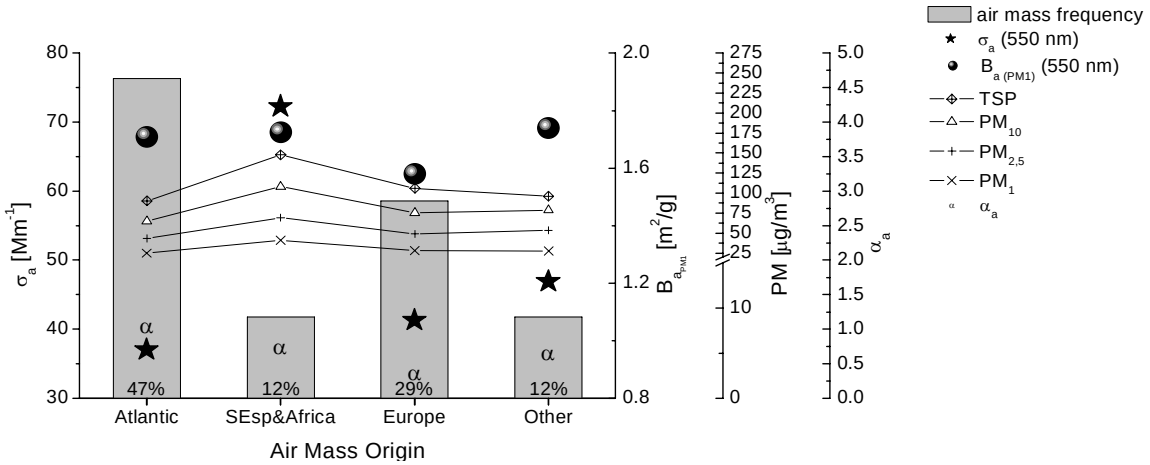


Fig.10. Classification of air masses according with its origin. Optical parameters and PM values observed in each situation. Percentage values refer the frequence of each air mass origin.

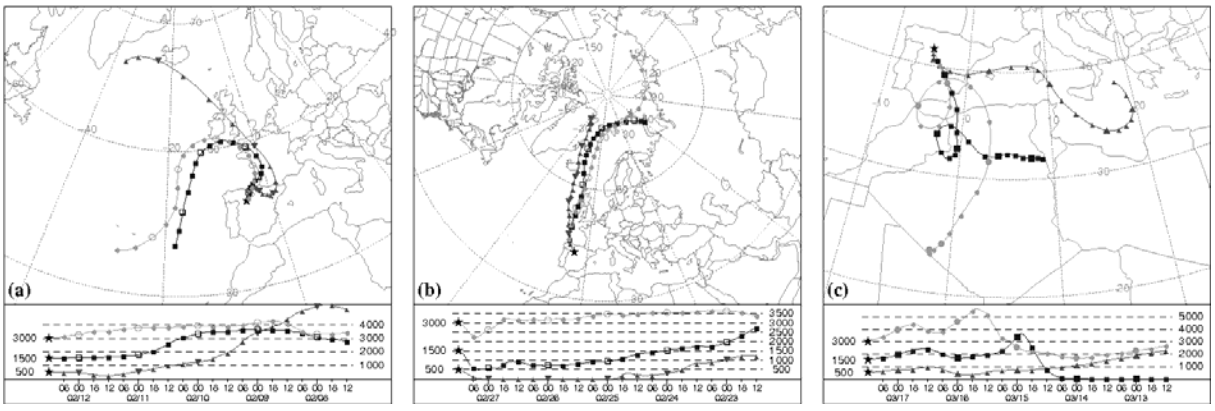


Fig.11. The trajectories of air masses for 500, 1500 and 3000 m above ground level. (a) Day of the highest absorption coefficient event, 12 Feb. Air masses backtracked to north Spain and France. (b) Day in which the lowest absorption coefficient was measured, 27 Feb. Air masses backtracked to the Arctic. (c) The trajectories of air masses at 17 Mar: Saharan dust event.

 © Sociedad Española de Óptica

550 nm) and the C/F ratio is 2.18. The PM1 = 31.69 μg/m$^3$, PM2.5 = 70.14 μg/m$^3$, PM10 = 100.80 μg/m$^3$ and TSP = 112.75 μg/m$^3$ levels are significantly higher than average.

One interesting feature is the highest PM events that occurred on 04 Feb and 31 Mar. The PM levels are high on both days but the other properties do not show relevant values. On 04 Feb the ratio C/F is lower than on 31 Mar, showing the presence of more fine particles and, the level of absorbent particles registered is higher with consequently higher absorption coefficients. On this day air masses had desertic origin but they had been recirculating over the Iberian Peninsula before they reach Valladolid. On 31 Mar the air masses had Atlantic origin (formed in Greenland) and reached Valladolid coming from Portugal, after which they reached the Peninsula from the southwest.

## 4. Summary and conclusions

We proposed in this study a combination of chemical, optical and other techniques in order to better characterize the atmospheric aerosols of a representative medium-sized town in north-central Spain (continental climate). The particulate matter levels were measured in four fractions and the chemical composition of each fraction was detailed as much as possible. In addition, the optical parameters as absorption coefficients, the alpha parameter of absorption and mass specific absorption coefficients were also determined. The trajectories of air masses were analyzed and combined with the measured parameters to further explore the possible sources.

The main findings of this study are: 1) the extremely high values of PM registered in Valladolid, that can be related with the local rough and dry soils and frequently with desert dust events; 2) the anticorrelation between $\sigma_a$ and C/F ratio, except during the desert dust events; 3) the increase of $\sigma_a$ values during desert events, which can be related with coagulation of small absorbent particles with dust, forming mixtures of stronger absorbent particles.

**Acknowledgements**

This study was carried out at the University of Valladolid, partially supported by research contract CYCIT Ref. REN2002-00966/CLI, while S. Mogo was on a PhD leave from the University of Beira Interior, Portugal. The authors gratefully acknowledge the NOAA Air Resources Laboratory (ARL) for provision of the HYSPLIT transport and dispersion model and the READY website used in this publication (www.arl.noaa.gov/ready.html).

 © Sociedad Española de Óptica